Spontaneous emission in ultracold spin-polarized anisotropic Fermi seas

Brian O'Sullivan* and Thomas Busch
Department of Physics, National University of Ireland, UCC, Cork, Republic of Ireland
(Received 2 October 2008; published 3 March 2009)

We examine and explain the spatial emission patterns of ultracold excited fermions in highly anisotropic trapping potentials in the presence of a spin-polarized Fermi sea of ground-state atoms. Due to the Pauli principle, the Fermi sea modifies the available phase space for the recoiling atom. This leads to the well-known modification of the atomic decay rate, but also to a spatial modulation in the probability of the emitted photon's direction. In this work we carry out the first detailed investigation into these spatial anisotropies and show that they are due to an intricate interplay between Fermi energies and degeneracy values of specific energy levels. We identify different regimes and show that the emission can be engineered to become highly directional. As the latter is usually only possible in cavity settings, our results describe an alternative idea for a directional photon source.

DOI: 10.1103/PhysRevA.79.033602 PACS number(s): 03.75.Ss, 05.30.−d, 67.85.Lm

I. INTRODUCTION

Cold samples of neutral fermionic atoms have become an important test bed for a large number of interesting phenomena in many-body physics [1]. Since the first realization of quantum degeneracy using two spin components of ^{40}K [2], the field has moved quickly from fundamental quantum statistical experiments [3] into other areas such as transitions from Bose-Einstein condensates (BEC) to BCS phases [4], solid-state physics [5], and even quark-gluon physics [6].

Today probably the most active areas of research into cold fermions are composite systems, where by pairing single atoms one can observe molecular BECs or superfluid BCS states. Besides molecular or Cooper pair physics, monoatomic gases have also shown a large potential for demonstrating new and exciting physics. While the most dramatic consequence of the antisymmetry condition on the wave function of identical fermions is the formation of the Fermi sea at low temperatures, other effects have been predicted and been observed. Among them are the modification of the scattering properties of two atoms, which leads to a reduced efficiency of evaporative cooling [7,8], narrowing of the line width of light propagating through the gas [9,10], and the suppression of off-resonant light scattering [11,12].

The inhibition of spontaneous emission in the presence of a ground-state Fermi sea is another fundamental prediction which results directly from the Pauli principle [12–14]. In it a degenerate Fermi sea of a spin-polarized gas forms the environment for a single excited atom of the same kind. Due to the Pauli principle, the Fermi sea effectively blocks out a large amount of the phase space that would otherwise be available to the excited atom after a de-excitation transition. This leads to a modification of the emission properties of the excited atom and the details of the effect are determined by the size of the Fermi sea, the system's temperature, and the anisotropy of the trap [14]. The influence on the lifetime of the excited atom has been recently exhaustively investigated [14] and the effect was shown to be an atom-optical analog of well-known effects in cavity QED [15].

In this work we will investigate the influence of the presence of a Fermi sea on the spatial distribution of the emission spectrum of a single atom in an anisotropic trap. The fact that the emission spectrum becomes anisotropic was first mentioned in [14,16] and simple explanations for this effect were given. Here we investigate the pattern formation in detail and in particular consider highly anisotropic traps, which can be achieved today by experimentally using, for example, optical lattices [17,18]. We will show that the involved effects can be understood by careful analysis of the underlying accessible mode structure.

In Sec. II we will first describe the model we are using and in Sec. III, derive a relation between the Fermi energy and the number of particles in an anisotropic trap. In Sec. IV we describe the effect of the anisotropy on the behavior of the individual transition elements for spontaneous emission and apply the results to explain the specifics of the overall emission pattern. Finally we conclude.

II. MODEL

We consider an ideal gas of spin-polarized fermions trapped in a harmonic potential. All atoms are assumed to be in their internal ground state, $|g\rangle$, so that the gas becomes quantum degenerate at low enough temperatures and forms a perfect Fermi sea at absolute zero. In the following we will restrict our calculations to this limit, as in it the effects we describe are most pronounced and the extension to finite temperatures is, while computationally challenging, conceptually straightforward.

In addition to the Fermi sea we assume the presence of a single extra fermion, which is distinguished from the others by being in an internally excited state $|e\rangle$. As above, and with the same implications for higher temperatures, we assume this particle to be in the motional ground state. After some time this atom will spontaneously emit a photon, make a transition into the ground state, and become part of the Fermi sea. As all atoms are assumed to be spin polarized, the Pauli principle demands that the new ground-state atom has to join the Fermi sea with an energy larger than the Fermi energy. This is an energetically very unfavorable process and the

*bosullivan@phys.ucc.ie

presence of the Fermi sea will therefore lead to an inhibition of the spontaneous emission rate with respect to the case of a free space particle [13,14]. In addition to the inhibition, the radial intensity distribution of the emission spectrum will also start to deviate from the single-particle isotropic shape and in the following we will investigate how the observed emission patterns arise.

In doing so, we will neglect the effects of reabsorption of the emitted photon. In fact, reabsorption can be seen as the same situation where a single atom in the ground state is excited by a weak laser pulse, which is a situation that was treated in [14] and for which it was shown that emission happens overwhelmingly in the forward direction, thereby not fundamentally affecting the results of this work.

In the following we will denote the spontaneous emission rate of photons along the direction Ω and into the solid angle $d\Omega$ in the presence of N ground-state fermions by $\Gamma(\Omega)d\Omega$ and compare it to the free case $(N=0)$ which we denote by $\Gamma_0(\Omega)d\Omega$. Using Fermi's golden rule we can express the excited atom's decay rate as

$$\frac{\Gamma(\Omega)}{\Gamma_0(\Omega)} = \sum_{\vec{n},\vec{m}=0}^{\infty} P_m(1-F_n)|\langle\vec{n}|e^{-i\vec{k}(\Omega)\cdot\vec{r}}|\vec{m}\rangle|^2, \tag{1}$$

where $F_n=(e^{(\hbar\omega/k_BT)(\vec{\lambda}\cdot\vec{n})}+1)^{-1}$ is the Fermi-Dirac distribution function and $(1-F_n)$ is the probability that an energy level $|n\rangle$ of the harmonic trap is unoccupied. $P_m=P_0e^{-(\hbar\omega/k_BT)\vec{\lambda}\cdot\vec{m}}$ is the Boltzmann distribution function describing the single excited fermion in state $|m\rangle$ of the harmonic trap, which in turn is assumed to have the frequencies $(\omega_x,\omega_y,\omega_z)\equiv\omega\vec{\lambda}$. If we restrict Eq. (1) to zero temperature the Fermi-Dirac distribution function becomes a step function and hence only states with an energy greater than the Fermi energy have a finite value for $1-F_n$. Similarly, the excited fermion will occupy the ground state of the harmonic trap, $|m\rangle=|0\rangle$, and Eq. (1) simplifies to

$$M_f(\Omega) = \frac{\Gamma(\Omega)}{\Gamma_0(\Omega)} = \sum_{n=n_F+1}^{\infty} |\langle\vec{n}|e^{-i\vec{k}(\Omega)\cdot\vec{r}}|0\rangle|^2, \tag{2}$$

where n_F represents the Fermi shell. The most well-known result originating from Eq. (1) is the inhibition of spontaneous emission by the excited atom [14]. However, the spatial emission probability is also known to become anisotropic [14,16] and in the following we will present a thorough and detailed investigation into this effect. This is of interest with regards to the new parameter ranges which have become experimentally available in recent years, which include lower and lower temperature Fermi gases and, in particular, highly anisotropic traps.

We assume that the harmonic-oscillator potential has the following standard form:

$$V = \frac{M\omega^2}{2}(\vec{\lambda}\cdot\vec{r})^2 = \frac{M\omega^2}{2}(\lambda_x^2x^2+\lambda_y^2y^2+\lambda_z^2z^2), \tag{3}$$

where M is the mass of the particle and the values of $\lambda_{x,y,z}$ determine the degree of anisotropy in the different directions. For numerical simplicity we will only deal with values of $\lambda\geq 1$ and restrict ourselves to two types of anisotropic trapping potentials in which two of the axes have identical strength

$$\lambda_x=\lambda_y=1 \quad \text{and} \quad \lambda_z=\lambda, \quad \text{pancake shape}, \tag{4a}$$

$$\lambda_x=\lambda_y=\lambda \quad \text{and} \quad \lambda_z=1, \quad \text{cigar shape}. \tag{4b}$$

Due to the symmetries of the pancake- and cigar-shaped traps about the tight and the soft axes, respectively, Eq. (2) can be simplified and expressed in terms of incomplete gamma functions for both trap shapes

$$M_f(\theta) = \frac{\gamma(n_F+1,\beta)}{\Gamma(n_F+1)} + e^{-\beta}\sum_{n=0}^{n_F}\frac{\beta^n}{n!}\frac{\gamma\left(\left\lfloor\frac{n_F-n}{\lambda}\right\rfloor+1,\frac{\alpha}{\lambda}\right)}{\Gamma\left(\left\lfloor\frac{n_F-n}{\lambda}\right\rfloor+1\right)}. \tag{5}$$

Here γ denotes the lower incomplete gamma function [19], $\lfloor x\rfloor$ denotes the largest integer less than or equal to x and n_F is the quantum number of the Fermi shell, i.e., the highest shell occupied by the Fermi sea. With this choice of notation, $n_F=0$ represents a trap in which solely the ground state is occupied. Therefore, the absence of any Fermi sea can be treated by setting $n_F=-1$ in the formulas below. For brevity we have defined

$$\alpha=\eta^2\cos^2\theta, \quad \beta=\eta^2\sin^2\theta \quad \text{pancake shape}, \tag{6a}$$

$$\alpha=\eta^2\sin^2\theta, \quad \beta=\eta^2\cos^2\theta \quad \text{cigar shape}, \tag{6b}$$

in which η represents the Lamb-Dicke parameter. One can immediately see that the angular distributions for the pancake- and the cigar-shaped traps can be obtained from each other by a simple spatial $\pi/2$ rotation, as one would expect. We will make use of this fact when discussing emission patterns in Sec. IV.

III. DEGENERACIES

Let us first discuss the relationships between the different parameters characterizing a Fermi sea in an anisotropic trap. Since the degeneracies of states with equal energy are a function of the trapping frequencies in the different directions, the relationship between the Fermi energy and particle number in an anisotropic potential is not as straightforward as in the well-known isotropic case [20].

The eigenenergies of the harmonic potential in Eq. (3) are given by

$$E_{n_p} = \left[n_p+\left(\frac{\lambda}{2}+1\right)\right]\hbar\omega, \tag{7a}$$

$$E_{n_c} = \left[n_c+\left(\lambda+\frac{1}{2}\right)\right]\hbar\omega, \tag{7b}$$

where we have defined the shell quantum numbers of the pancake- and cigar-shaped harmonic traps as $n_p=n_x+n_y+\lambda n_z$ and $n_c=\lambda n_x+\lambda n_y+n_z$, respectively. As usual, n_x, n_y, and n_z refer to the integer quantum numbers of the harmonic oscillator.

As the aspect ratio of a trapping potential is increased the resulting energy levels typically have a reduced degeneracy relative to the isotropic case $\lambda=1$ [21]. For the purposes of this work, and without loss of generality, we will consider only integer values of λ, allowing us in turn to restrict ourselves to integer values for $n_{p,c}$. Therefore we can write the degeneracy for states with fixed energy as

$$g_{n_p} = \frac{1}{2}(\tilde{n}_p + 1)(2n_p - \lambda\tilde{n}_p + 2), \tag{8a}$$

$$g_{n_c} = \frac{1}{2}(\tilde{n}_c + 1)(\tilde{n}_c + 2), \tag{8b}$$

where here and in the following all quantities carrying a tilde take the value of the quantity without the tilde divided by λ and rounded down to the nearest integer, i.e., $\tilde{x}=\lfloor x/\lambda \rfloor$. Consequently, the total number of quantum states with an energy equal to and smaller than E_{n_F} is then given by the sum

$$S = \sum_{n=0}^{n_F} g_n, \tag{9}$$

which can be calculated to be given by

$$S_p = \frac{1}{6}(\tilde{n}_F + 1)(2n_F - \lambda\tilde{n}_F + 2) \times \left(\frac{3}{2}n_F - \frac{3}{4}\lambda\tilde{n}_F + \frac{\lambda^2\tilde{n}_F(2+\tilde{n}_F)}{8+8n_F-4\lambda\tilde{n}_F} + 3\right), \tag{10a}$$

$$S_c = \frac{1}{6}(\tilde{n}_F + 1)(\tilde{n}_F + 2)(3n_F - 2\tilde{n}_F\lambda + 3). \tag{10b}$$

In our model we assume a spin-polarized gas in which each oscillator state is filled with one fermion only. Equation (9) therefore determines the number of particles confined for a given Fermi energy $E_F=n_F\hbar\omega+E_G$, where E_G is the ground-state energy of the potential.

IV. EMISSION PATTERNS IN ANISOTROPIC TRAPS

A. Emission probabilities

To understand the emission patterns later on, let us first have a brief look at the emission probabilities of an excited atom in an anisotropic trap. In the presence of an anisotropic Fermi sea the rate of spontaneous emission along a specific direction is determined by three parameters: (1) the number of ground-state atoms, (2) the degeneracy of the available states, and (3) the Lamb-Dicke parameter $\eta=\sqrt{E_R/\hbar\omega}$. The latter determines the range of accessible states and is given by the ratio between the recoil energy, $E_R=\hbar^2k_0^2/2M$, and the trapping strength, $\hbar\omega_{x,y,z}$, in the different directions. Here k_0 is the wave vector corresponding to the transition $|e\rangle \rightarrow |g\rangle$.

In this section we will focus on the influence of the degeneracies of the available states and therefore on the anisotropy of the trap. Let us do this by examining the matrix elements for individual transitions from the ground center-of-mass state of the excited atom to a single final state, $|n\rangle$,

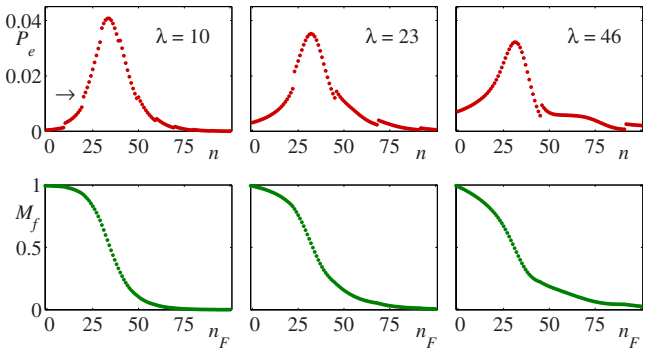

FIG. 1. (Color online) Top row: emission probability, P_e, into individual shells in a pancake-shaped trap for $\eta^2=36$ and $\lambda=10,23,46$. Arrow indicates the $n=20$ energy level of the harmonic trap, which is referred to in the text. Bottom row: decay rate of the excited particle, M_f, for the same parameters as above.

$$P_e(n) = |\langle n|e^{ikx}|0\rangle|^2. \tag{11}$$

For an isotropic trap this is a continuous distribution of finite width which is centered around the energy level $n=\eta^2$. The effects introduced by an anisotropy are significant and can be clearly seen in the graphs in the upper rows of Figs. 1 and 2, where we show P_e for a pancake- and a cigar-shaped traps, respectively, for increasing values of the anisotropy $\lambda=10$, 23, and 46. The most obvious feature in both situations is the appearance of a λ-dependent discontinuity in the distribution, which is more pronounced in the cigar-shaped setting.

To explain this behavior, let us first intuitively argue its existence. When an internally excited atom which is trapped in the ground state of an empty isotropic harmonic trap decays, the probability of the photon being emitted is the same in all directions. This is rather easy to understand as in this situation the density of states is identical in all directions. However, for the anisotropic trap the situation is different. As the aspect ratio is increased, the degeneracy of any energy level will either decrease or remain the same. Therefore, up to a specific shell the number of quantum states, as given by Eqs. (10a) and (10b), will be reduced and, as a result, the density of states in the different directions changes. Since the

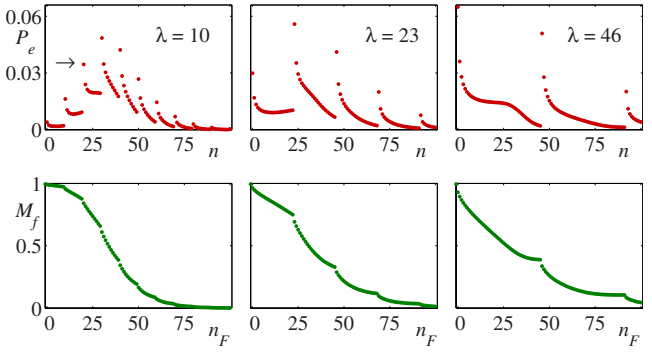

FIG. 2. (Color online) Top row: emission probability, P_e, into individual shells in a cigar-shaped trap for $\eta^2=36$ and $\lambda=10,23,46$. Arrow indicates the $n=20$ energy level of the harmonic trap, which is referred to in the text. Bottom row: decay rate of the excited particle, M_f, for the same parameters as above.

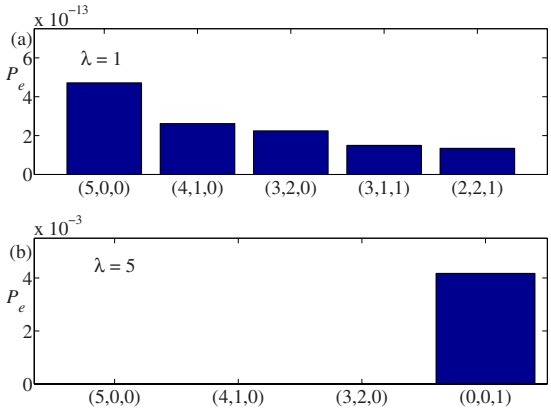

FIG. 3. (Color online) (a) Emission probability into individual states within the shell $n=5$ in an isotropic trap. The triplets represent (n_x,n_y,n_z) and all permutations of each triplet have the same probability. The Lamb-Dicke factor is $\eta=5$, however changing this value only scales all values. (b) Emission probability into individual states within the shell $n=5$ in a pancake trap with $\lambda=5$. The values for the three states on the left are not visible on this scale.

recoil of the de-excited fermion to a certain quantum state and the direction of the emitted photon are directly related, it seems rather surprising that for the free case this emission remains isotropic irrespective of the diminishing number of quantum states. However, it is exactly the modified distribution shown in the upper rows in Figs. 1 and 2 that makes this phenomenon possible.

To gain more insights into the source of the discontinuities let us consider the emission probability into specific states within a degenerate shell n of an isotropic and a pancake-shaped ($\lambda=5$) trap. Figure 3 shows $P_e(n_x,n_y,n_z)$ for a fixed shell, in which all combinations of the triplet [in both (a) and (b)] of quantum numbers adds up to $n=5$. It can be seen that in general states which include ground-state excitations have a higher probability for occupation than the ones which do not, which is due to the fact that the excited atom is initially in its center-of-mass ground state.

When we move from the isotropic to the anisotropic setting it is therefore clear that whenever the value of an energy shell, n, reaches an integer multiple of the anisotropy parameter, the shell contains a state with two ground-state excitations. As these states have a higher probability of occupation [see Fig. 3(b)] the overall emission probability into this energy shell is increased, leading to the observed discontinuous jump. As an example let us consider a pancake-shaped trap with an aspect ratio of $\lambda=10$. For the shell $n=19$ the degenerate states are $(n_x+n_y,n_z)=(19,0)$ and (9, 1), whereas for the $n=20$ energy level (indicated by the arrow in Fig. 1) the states are $(n_x+n_y,n_z)=(20,0)$, (10, 1), and (0, 2). The *extra* (0, 2) state is the dominant contributor and its appearance is responsible for the discontinuous increase in the emission probability. For the cigar trap this effect is even more pronounced as there are two tight directions and in the example above the states $(n_x,n_y,n_z)=(2,0,0)$ and (0, 2, 0) become both available. Closer examination shows that the state (1, 1, 0) also gives a large (but smaller) contribution to emission into the $n=20$ shell, followed by the (1, 0, 10) state, whereas the (0, 0, 20) state's occupation probability is negligible.

Transitions into states including a ground-state excitation just have a larger overlap with the initial state and are therefore more likely. In this respect, a transition into a state with two ground-state excitations combined with a small change in the principle quantum number contributes to the high probability of the state's occupation. The smallest change in principle quantum number is in the tight direction, therefore making transition into states with low tight excitations >0 and low soft excitations ≈ 0 more likely. This is in contrast to states with high soft excitations and ground-state tight excitations which are unlikely candidates for occupation.

For completeness we show the integrated emission probability for increasing particle number (i.e., increasing Fermi energy or Fermi level) and different anisotropies in bottom rows of Figs. 1 and 2. Fermi inhibition is absent for the empty trap ($M_f=1$), shown for $n_F=-1$, slowly increases for $n_F\geq 0$, and accelerates for $n_F\sim \eta^2$. The discontinuity in the variable $P_e(n)$ translates clearly into nonsmooth kinks in this distribution.

B. Emission along tight and soft axes

The fact that the presence of an anisotropic Fermi sea will lead to anisotropic emission patterns was already noted in [14,16] and in the following we will develop a detailed understanding of the directional features. Since for the pancake- as well as for the cigar-shaped trap the emission is isotropic around their respective symmetry axis, $(0,\pi)$, we can treat both geometries in a quasi-two-dimensional (quasi-2D) picture. It is then immediately clear that the results for both settings will be related by a simple $\pi/2$ rotation (due to our definition of $\lambda\geq 1$).

Let us first look at the emission along the principal axes of the anisotropic trap in the tight and the soft directions. Choosing the tight direction in the pancake- (cigar-) shaped trap along $\theta=0$ ($\theta=\pi/2$) the modification factor in Eq. (5) simplifies to

$$M_f=\frac{\gamma\left(\tilde{n}_F+1,\frac{\eta^2}{\lambda}\right)}{\Gamma(\tilde{n}_F+1)}. \tag{12}$$

The behavior of this equation with increasing anisotropy is shown in Fig. 4 for a system with $n_F=60$. The most obvious feature of the plot is a series of sawtooth-like discontinuities. Careful examination shows that n_F of these exist and they appear whenever the value of the aspect ratio, λ, increases beyond the values of $\frac{n_F}{m}$, $(m=1,2,\ldots,n_F)$. The increase in emission probability for values just after these points is due to the availability of an extra free state with a lower tight excitation just outside the Fermi edge. For example, in the pancake trap, when one moves from $\lambda=30$ to $\lambda>30$ the state $(n_x+n_y,n_z)=(0,2)$ emerges from the Fermi sea for $n_F=60$. As discussed in Sec. IV A, this state has a high probability to be emitted into as it contains ground-state excitations in the soft direction, hence the large increase in the decay rate. By increasing λ further this state moves away from the Fermi edge and the emission probability decreases until the next state with a lower tight excitation emerges from the Fermi

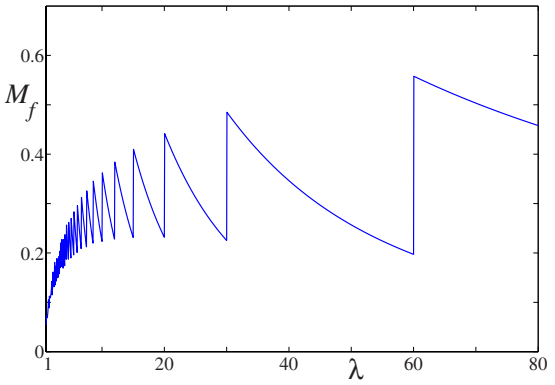

FIG. 4. (Color online) M_f along the tight axis at $T=0$. $\eta^2=49$ and $n_F=60$. Note that we use a continuous distribution of λ for this graph.

sea. For values of $\lambda > n_F$ no more discontinuities appear since the Fermi sea only occupies energy states with ground-state excitations in the tight direction. Emission along the soft direction can be calculated from Eq. (12) by taking $\lambda=1$ and the decay rate along this direction is determined exclusively by the Fermi shell n_F and the value of the Lamb-Dicke parameter η.

Considering a fixed value of the aspect ratio λ in either anisotropic trapping potential and changing n_F one notices a degeneracy in the emission probability in the tight direction [shown in Fig. 5(a)]. This behavior was already mentioned in [14] and we can see from Eq. (12) that it stems from the fact that $\tilde{n}_F$ only changes its value in steps of λ. An increase in the value of $\tilde{n}_F$ coincides with the Fermi sea occupying a state with a higher tight excitation (and ground-state soft excitations), leading to a decrease in the decay rate along the tight direction. For example, when moving from $n_F=35$ to $n_F=36$ the state $(n_x+n_y,n_z)=(0,9)$ becomes occupied by the Fermi sea, producing the discontinuous reduction of the decay rate [see Fig. 5(a)].

C. Fine structure

The emission spectrum between the principal axes is characterized by the appearance of a fine structure [see Fig. 5(b)], which exists for a wide range of parameters. The first hint to

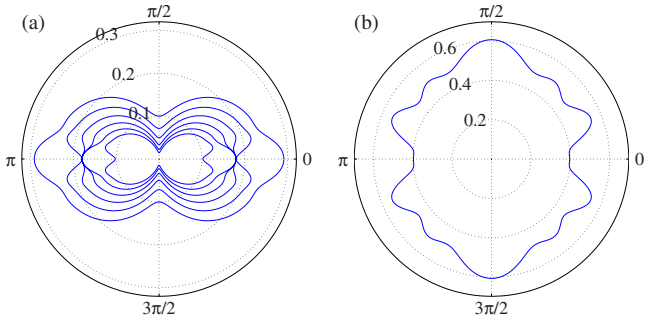

FIG. 5. (Color online) (a) $M_f(\theta)$ in a pancake-shaped trap at $T=0$. $\eta^2=25$ and $\lambda=4$ with $n_F=31$ (outermost) to $n_F=36$ (innermost). (b) $M_f(\theta)$ in a pancake-shaped trap with $\lambda=11$, $\eta^2=25$, and $n_F=23$.

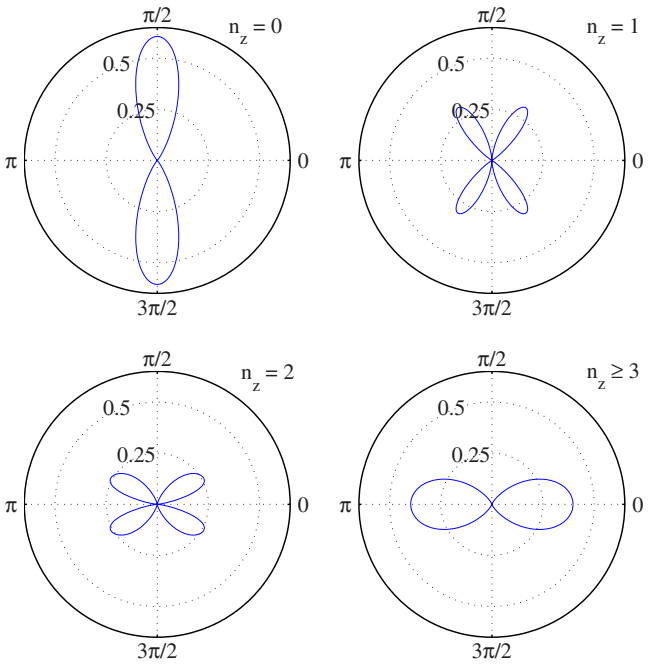

FIG. 6. (Color online) $M_f(\theta,n_z)$ for a pancake-shaped trap, with $\lambda=11$, $\eta^2=25$, and $n_F=23$. In the four graphs the decay is only allowed into quantum states of the harmonic trap with $n_z=0$, 1, 2, and $n_z \geq 3$, respectively.

understanding the origins of the visible extrema comes from noticing that the number of maxima between the soft and tight axes is related to the number of excitations in the tight direction that are occupied by the Fermi sea $\tilde{n}_F$. To show this relation let us consider the emission probability into shells with a fixed value for n_z in a pancake-shaped trap

$$M_f(\theta,n_z) = e^{-\alpha/\lambda} \frac{\left(\frac{\eta^2}{\lambda}\right)^{n_z}}{n_z!} \frac{\gamma(\max(0,n_F-\lambda n_z+1),\beta)}{\Gamma(\max(0,n_F-\lambda n_z+1))}, \tag{13}$$

with the definition of α and β given in Eq. (5). As a specific example we show in Fig. 5(b) a gas with $n_F=23$, $\eta^2=25$, and $\lambda=11$. In this case we find $\tilde{n}_F=2$ maxima in the $\pi/2$ arc between the tight to the soft axis. Comparing this emission pattern to the results from Eq. (13), one can see (Fig. 6) that each isolated contribution from a transition into a state with a fixed value of n_z is responsible for one of the maxima. For values of $n_z > \tilde{n}_F$ the emission is predominantly into the tight direction, therefore originating from transitions into states for which both ground-state excitations in the soft direction are available. Similarly, when restricting the recoiling atom to occupying states with a ground-state excitation in the tight direction, $n_z=0$, the emission is mainly focused around small angles about the soft axis. The intermediate excitations, $n_z=1,2$, make up the two intermediate ripples between the principle axes and summing up the contributions to the photon emission of all four plots in Fig. 6 gives the emission plot shown in Fig. 5(b). In contrast, if we calculate Eq. (13) for an isotropic trap for different values of n_z, each individual term

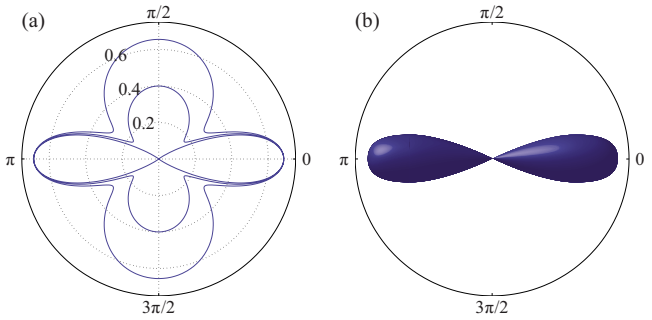

FIG. 7. (Color online) (a) $M_f(\theta)$ in a cigar-shaped trap at $T=0$, with $n_F=45$ and $\eta^2=49$. $\lambda=46$ (outermost), $\lambda=96$ (center plot), and $\lambda=\infty$ (innermost). The plot is symmetric through a 2π rotation about the $(0,\pi)$ axis. (b) A three-dimensional illustration of the excited particles decay rate in a cigar trap in the large anisotropy limit.

would show a similar behavior of having a single maximum at a finite angle between the principle axes. However, the sum of those will give the isotropic emission pattern which corresponds to the decay rate being the same in all directions.

It is now obvious that for the limit $\lambda > n_F$ the fine structure disappears and the extrema of emission will be located around the directions of the principal axes [see Fig. 7(a)]. As $\lambda \to \infty$, emission into the tight direction is reduced, whereas the emission in the soft direction [$(0,\pi)$ axis for the cigar trap] remains constant [Fig. 7(b)]. In this regime the Fermi sea is completely confined to states with ground-state excitations in the tight direction. Therefore, it becomes easier for the recoiling atom to access states in the soft direction due to the diminishing density of states in the tight direction. In the limit of $\lambda \to \infty$ the emission probability can be written as

$$M_f(\theta;\lambda \to \infty) = \frac{\gamma(n_F+1,\beta)}{\Gamma(n_F+1)}, \tag{14}$$

and it shows that the emission probability in the tight direction has completely vanished.

It is possible to make use of this behavior and create a system where photon emission becomes highly directional. While directional photon emission is usually achieved by using optical cavities (and therefore engineering the Hilbert space of the photon), this example is complementary in that it uses a cavity (trap) for the atoms and thereby engineers the Hilbert space of the particles. Let us stress that it is not primarily the size of the Fermi sea that is responsible for this effect, merely the presence of the Fermi sea. The strength of the effect is therefore independent of the strength of the inhibition effect uncovered earlier and the emission probability of the photon in the presence of a Fermi sea can still be close to the emission probability in free space while $\eta^2 \gtrsim n_F$ [see Fig. 7(a)]. As the emission is symmetric through a 2π rotation about the $(0,\pi)$ axis in the above example, we display the three-dimensional (3D) emission probability in Fig. 7(b). Also note that for a pancake-shaped trap this effect would correspond to emission into a well-defined plane perpendicular to the tight principal axis.

V. CONCLUSION

In this work we have given a detailed investigation into the spatial properties of spontaneous emission of a single atom in the presence of an anisotropic, ideal, and spin-polarized ultracold Fermi gas. The demand to obey the Pauli principle leads to the formation of a nontrivial anisotropic emission pattern for the photon, which can be explained by carefully examining the allowed transitions the recoiling atom can make. To do this we have made several simplifying assumptions, which however were only operational in nature and do not affect the basic phenomena uncovered.

We have first calculated the relation between the Fermi energy and particle number for cigar- as well as pancake-shaped geometries as a function of the aspect ratio strength. We then investigated the single-particle transition matrix element for both geometries of anisotropic traps. The change in the density of states in the different spatial directions was found to be accompanied by the appearance of discontinuities in the distribution of the emission probability spectrum for different shells. While in an isotropic trap these two effects cancel and produce an isotropic emission spectrum; in an anisotropic trap they lead to an intricate fine structure in the presence of a Fermi sea.

In a next step we have explained this fine structure by attributing the extrema to the emissions which come from the transitions of the recoiling atom into well-defined states in the tight direction. We also showed that if the aspect ratio exceeds the Fermi shell, the fine structure vanishes and the emission spectrum becomes smooth, though not isotropic, again.

Finally, we have pointed out that this system can be used to create a highly directional photon source. The effect uncovered is complementary to the common use of optical cavities to influence a photons direction after emission and makes use of the ability to influence the atom's phase space. All effects described in this work rely on the existence of a degenerate Fermi sea to engineer the atomic center-of-mass Hilbert space. In contrast an ideal Bose gas would always have the full Hilbert space available, thus exhibiting isotropic emission. Therefore an experimental observation of directional photon emission in anisotropic cold fermionic gases would be a sign of the fundamental consequences of the antisymmetry of fermionic particles.

ACKNOWLEDGMENTS

We would like to thank Tomás Ramos for valuable discussions. This project was supported by Science Foundation Ireland under Project No. 05/IN/I852. B.O.S. acknowledges support from IRCSET through the Embark Initiative No. RS/2006/172.

[1] S. Giorgini, L. P. Pitaevskii, and S. Stringari, Rev. Mod. Phys. **80**, 1215 (2008).
[2] B. DeMarco and D. S. Jin, Science **285**, 1703 (1999).
[3] A. G. Truscott, K. E. Strecker, W. I. McAlexander, G. B. Partridge, and R. G. Hulet, Science **291**, 2570 (2001).
[4] W. Ketterle and M. W. Zwierlein, *Ultracold Fermi Gases*, Proceedings of the International School of Physics "Enrico Fermi," Course CLXIV, Varenna, 2008, edited by M. Inguscio, W. Ketterle, and C. Salomon (IOS, Amsterdam, 2008).
[5] I. Bloch, J. Dalibard, and W. Zwerger, Rev. Mod. Phys. **80**, 885 (2008).
[6] E. V. Shuryak, Nucl. Phys. A. **750**, 64 (2005).
[7] G. Ferrari, Phys. Rev. A **59**, R4125 (1999).
[8] B. DeMarco, S. B. Papp, and D. S. Jin, Phys. Rev. Lett. **86**, 5409 (2001).
[9] J. Ruostekoski and J. Javanainen, Phys. Rev. Lett. **82**, 4741 (1999).
[10] J. Javanainen, J. Ruostekoski, B. Vestergaard, and M. R. Francis, Phys. Rev. A **59**, 649 (1999).
[11] B. DeMarco and D. S. Jin, Phys. Rev. A **58**, R4267 (1998).
[12] A. Görlitz, A.P. Chikkatur, and W. Ketterle, Phys. Rev. A **63**, 041601(R) (2001).
[13] K. Helmerson, M. Xiao, and D. Pritchard, *IQEC'90, Book of Abstracts*, QTHH4 (1990).
[14] Th. Busch, J. R. Anglin, J. I. Cirac, and P. Zoller, Europhys. Lett. **44**, 1 (1998).
[15] E. M. Purcell, Phys. Rev. **69**, 681 (1946).
[16] J. Javanainen and J. Ruostekoski, Phys. Rev. A **52**, 3033 (1995).
[17] G. Modugno, F. Ferlaino, R. Heidemann, G. Roati, and M. Inguscio, Phys. Rev. A **68**, 011601(R) (2003).
[18] H. Moritz, T. Stöferle, K. Günter, M. Köhl, and T. Esslinger, Phys. Rev. Lett. **94**, 210401 (2005).
[19] M. Abramowitz and I. Stegun, *Handbook of Mathematical Functions* (Dover, New York, 1964).
[20] J. Schneider and H. Wallis, Phys. Rev. A **57**, 1253 (1998).
[21] C. Cohen-Tannoudji, B. Diu, and F. Laloë, *Quantum Mechanics* (Wiley, New York, 1977), Vol. 1, p. 550.